Engineering Analysis of Slender-Body Aerodynamics Using Sychev Similarity Parameters

Michael J. Hemsch*
PRC Aerospace Technologies Division, Hampton, Virginia

The similarity parameters deduced by V. V. Sychev for inviscid hypersonic flow over slender bodies are reviewed and used to correlate flowfield, surface-pressure, normal-force, and center-of-pressure data for supersonic flow over thin slender wings and smooth slender bodies at low-to-high angles of attack. Although Sychev expected similarity to hold only for hypersonic freestream and crossflows, it is demonstrated empirically that similarity holds for any value of crossflow Mach number if the axial flow component is supersonic. It is shown for thin wings that similarity holds for much larger values of aspect ratio than Sychev supposed. One-term power-law expressions are found to fit all of the normal-force and center-of-pressure correlations, which suggests that it may be possible to develop a simple semiempirical method for estimating the aerodynamic characteristics of arbitrary slender airframes.

Nomenclature

A = power-law coefficient for normal force
AR = aspect ratio
B = power-law exponent for normal force
b = span
C = power-law coefficient for axial location of center of pressure
C_m = pitching-moment coefficient referred to planform area and body length
C_N = normal-force coefficient referred to planform area
c_p = pressure coefficient
c_r = centerline chord
c_t = tip chord
D = power-law exponent for axial location of center of pressure
E = power-law coefficient for lateral location of center of pressure
F = power-law exponent for lateral location of center of pressure
k_1 = similarity parameter, $\delta \cot\alpha$
k_2 = similarity parameter (crossflow Mach number), $M_\infty \sin\alpha$
k_3 = similarity parameter, $\tan\alpha/AR$
ℓ = body or wing length
M_∞ = freestream Mach number
n = power-law exponent for body planform
p = static pressure
p' = nondimensionalized static pressure, $p/q_\infty \sin^2\alpha$
p_∞ = freestream static pressure
q_∞ = freestream dynamic pressure
s = semispan
t_{max} = maximum wing thickness
u,v,w = flow velocity components in cylindrical coordinates
u',v',w' = nondimensional flow velocity components, $u/U_\infty \cos\alpha$, $v/U_\infty \sin\alpha$, $w/U_\infty \sin\alpha$, respectively
U_∞ = freestream velocity
x,r,ϕ = cylindrical coordinates aligned with the body axis with origin at nose tip
x',r',ϕ' = nondimensionalized coordinates, x/ℓ, r/b, ϕ, respectively
$\bar{x}$ = axial location of the center of pressure
$\bar{y}$ = spanwise location of the center of pressure
α = angle of attack
δ = slenderness parameter, b/ℓ
ε = ellipticity
θ_w = half-angle of wedge leading edge
λ = taper ratio, c_t/c_r
ρ = density
ρ' = nondimensional density, ρ/ρ_∞
ρ_∞ = freestream density

Presented as Paper 87-0267 at the AIAA 25th Aerospace Sciences Meeting, Reno, NV, Jan. 12–15, 1987; submitted Feb. 20, 1987; revision received July 20, 1987.

*Engineering Specialist. Associate Fellow AIAA.

Introduction

HIGHLY blended slender airframes with arbitrary cross-sectional shapes are promising candidates for high-performance tactical missiles, advanced fighter forebodies, hypersonic transports, and single-stage-to-orbit launch vehicles. The simultaneous constraints of volume, drag, stealth, lift, and static and dynamic stability characteristics make it necessary to use intuitive models to sort through the huge design space available. Unfortunately, the present lack of such models prevents full utilization of the design freedom afforded by arbitrary slender shapes. Engineering methods based on Newtonian impact theory[1] and an ad hoc combination[2-4] of slender-body theory,[5] H. Allen's crossflow drag theory,[6] and impact theory have been developed. However, they appear to be applicable primarily to high-fineness-ratio bodies whose cross sections are nearly axisymmetric. Any deviation from such a shape seems to require significant additional empiricism.

The work described herein was undertaken to develop a basis for engineering design tools suitable for all speeds and angles of attack for which the flow is quasisteady. The approach is based on the similarity analysis done by V. V. Sychev[7] for his development of hypersonic slender-body theory for arbitrary angles of attack. In the main body of the article, it is shown that Sychev's similarity appears to hold not only for hypersonic flows but for all flows over sufficiently slender bodies for which the axial Mach number is supersonic.

Sychev's results are presented first, together with comments on previous work. Next, it is shown that the parameters can be used to correlate flowfield characteristics and surface pressure data for thin delta wings. Normal-force and center-of-pressure correlations are then presented for three families of sharp-edged wings and two families of bodies with elliptical cross sections. It is noted that one-term power-law expressions fit all of the normal-force and center-of-pressure correlations. The coefficients and exponents of those expressions for the wings and bodies considered are examined together with their asymptotic limits. All of the correlations are for supersonic flows.

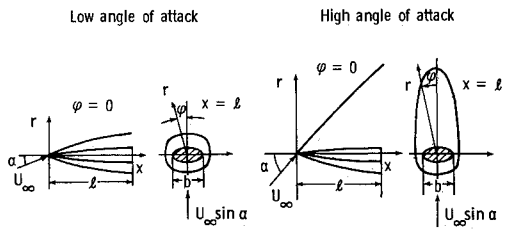

Fig. 1 Shock shape and coordinate system.

Hypersonic Similarity for Arbitrary Angles of Attack

In his analysis[7] of the Euler equations for hypersonic flow about an arbitrary slender body at an arbitrary angle of attack, Sychev assumed that

$$\delta = (b/\ell) \ll 1 \tag{1a}$$

$$M_\infty \delta > 1 \tag{1b}$$

$$M_\infty \sin\alpha \gg 1 \tag{1c}$$

where b is the body span and ℓ is the body length. Obviously, these conditions require that the freestream and crossflow Mach numbers be hypersonic. For small angles of attack (Fig. 1a), the flow disturbances are confined to a region near the body by the highly swept bow shock wave, thus satisfying Eq. (1a) in the flowfield. For high angles of attack (Fig. 1b), the disturbance field on the compression side of the body will again be confined to a region near the body. But on the leeside, the disturbance field will extend a considerable distance. However, Sychev reasoned that the leeside field contributes only weakly to the overall loading as long as the compression surface loading is sufficiently high. Hence, the flowfield disturbances of interest are close to the body, even for high angles of attack. Barnwell has pointed out[8] that Eq. (1c) is really too strong and that

$$M_\infty \sin\alpha > 1 \tag{2}$$

is a sufficient condition.

It will be shown later that the hypersonic parameters can be used to correlate experimental data for flows with low-to-moderate supersonic freestream Mach numbers and crossflow Mach numbers less than one. This extension of the range of applicability of hypersonic similarity appears to be due, at least in part, to the appearance of slender vortical flow near the leeside of the body, which again confines the disturbance field of interest to a region close to the body. Since the body and flowfield of interest are slender, Sychev introduced the following dimensionless independent variables in cylindrical coordinates:

$$x' = x/\ell \tag{3a}$$

$$r' = r/b \tag{3b}$$

$$\phi' = \phi \tag{3c}$$

and the dimensionless dependent variables

$$u' = u/U_\infty \cos\alpha \tag{4a}$$

$$v' = v/U_\infty \sin\alpha \tag{4b}$$

$$w' = w/U_\infty \sin\alpha \tag{4c}$$

$$p' = p/q_\infty \sin^2\alpha \tag{4d}$$

$$\rho' = \rho/\rho_\infty \tag{4e}$$

All of the dimensionless variables are of order one. By substituting Eqs. (3) and (4) into the governing Euler equations and shock conditions and then dropping higher-order terms, Sychev obtained an approximate set of equations and conditions representing a two-dimensional flow that is time-like in the axial direction. For a perfect gas, the approximate relations involve only the parameters

$$k_1 = \delta \cot\alpha \tag{5a}$$

$$k_2 = M_\infty \sin\alpha \tag{5b}$$

and the ratio of specific heats, which demonstrates for affine bodies in the same perfect gas that all of the dimensionless dependent variables are equal at corresponding points of the field if the similarity parameters k_1 and k_2 have the same values for the two cases. For example, since we have

$$p' = p'(x',r',\phi',k_1,k_2) \tag{6}$$

it is easy to show for perfect gases that p/p_∞ and $c_p/\sin^2\alpha$ are also similarity variables and are functions only of x',r',ϕ',k_1, and k_2.

Integrating the pressure over the body surface gives

$$\frac{C_N}{\sin^2\alpha} = f_1(k_1,k_2) \tag{7}$$

$$\frac{C_m}{\sin^2\alpha} = g_1(k_1,k_2) \tag{8}$$

These relations are somewhat inconvenient since the left-hand sides tend to infinity for small angles of attack. It is also more convenient for comparison of different families of affine bodies to use the parameter

$$k_3 = \frac{\tan\alpha}{AR} = \frac{\text{const}}{k_1} \tag{9}$$

Multiplying Eq. (7) by k_3 and replacing k_1 with k_3, we have the more convenient result

$$\frac{C_N}{AR \sin\alpha \cos\alpha} = f_2(k_2,k_3) \tag{10}$$

and dividing Eq. (8) by Eq. (7) gives

$$(\bar{x}/\ell) = g_2(k_2,k_3) \tag{11}$$

$$(\bar{y}/\ell) = h(k_2,k_3) \tag{12}$$

Equations (10–12) will prove particularly useful for correlating experimental data.

It should be noted that the preceding similarity rules were derived from the Euler equations. Hence, in order for the rules to hold, the flows of interest must be, at most, weakly dependent on Reynolds number. This is certainly the case for the flows examined herein.

Relationship with Previous Work

Small-Disturbance Theory

Multiplying Eqs. (7) and (8) by the square of k_2 gives

$$M_\infty^2 C_N = f(k_1,k_2) \tag{13}$$

$$M_\infty^2 C_m = g_3(k_1,k_2) \tag{14}$$

For small angles of attack,

$$k_1 \to \delta/\alpha \tag{15}$$

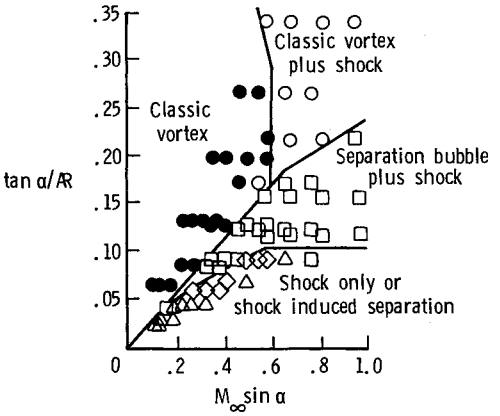

Fig. 2 Classification of Miller-Wood delta wing flowfield data[13] using the Sychev similarity parameters.

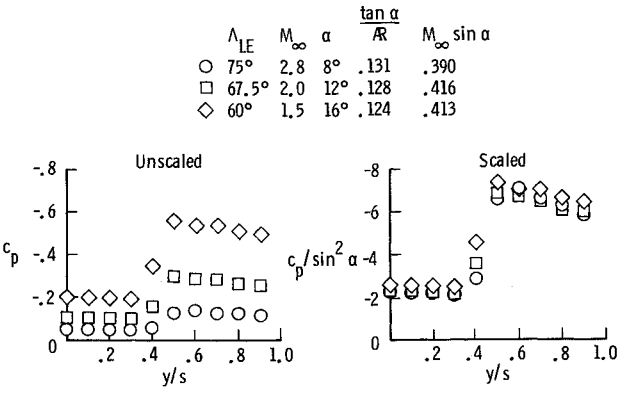

Fig. 3 Correlation of Miller-Wood leeside pressure data[13] for classical vortex case.

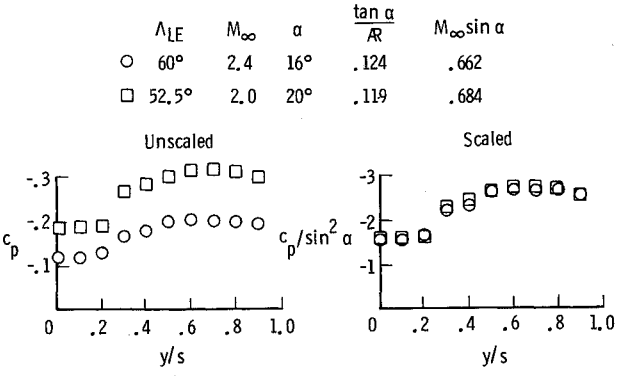

Fig. 4 Correlation of Miller-Wood leeside pressure data[13] for separation-bubble-plus-shock case.

$$k_2 \rightarrow M_\infty \alpha \tag{16}$$

Hence, for small angles of attack, we can combine k_1 and k_2 to get an alternate similarity parameter, $M_\infty \delta$, and Eqs. (13) and (14) reduce to

$$M_\infty^2 C_N = f_4(M_\infty \delta, M_\infty \alpha) \tag{17}$$

$$M_\infty^2 C_m = g_4(M_\infty \delta, M_\infty \alpha) \tag{18}$$

which is the form presented by Tsien[9] (see also Refs. 10 and 11).

Similarity Parameters

The similarity parameters $k_2 = M_\infty \sin\alpha$ and $k_3 = \tan\alpha/A\!R$ have been used separately in previous work but not together except for Sychev's analysis.[7] The crossflow Mach number has been used as part of crossflow drag theory to study flow over inclined bodies of revolution of high-fineness ratio since the beginning of the postwar missile era (e.g. see Refs. 2 and 6). The parameter $\tan\alpha/A\!R$ has appeared primarily in the work of J. H. B. Smith and his co-workers in their slender-body-theory studies of leading-edge vortices over slender wings (e.g., see Ref. 12). In slender-body theory, k_2 does not appear, and for small angles, Eq. (10) reduces to

$$\frac{C_N}{\alpha A\!R} = f_5(\alpha/A\!R) \tag{19}$$

Equation (19) is the form used by Smith,[12] although it can be shown that the slender-body governing equations lead in general to the full trigonometric form of Eq. (10).

Flowfield State and Surface-Pressure Correlations

In a recent extensive experimental investigation, Miller and Wood[13] were able to show that leeside flows over thin sharp-edged delta wings could be classified into several distinct types, depending on the flow mechanisms observed (e.g., shock or shockless, attached or separated, etc.). In addition, they developed a chart that clearly shows that the appearance of a flow type is dependent on the angle of attack normal to the leading edge and the component of Mach number normal to the leading edge. Their data were obtained for Mach numbers from 1.7–2.8 and for aspect ratios from 1.07–3.07. The angle-of-attack range was from 0–20 deg; hence, the crossflow Mach number was always subsonic.

If Sychev similarity holds for $M_\infty \sin\alpha < 1$, it should be possible to replot the Miller and Woods chart with k_2 and k_3 as the coordinates. The result is given in Fig. 2, showing that the similarity parameters can be used to define the flow-type domains.

Miller and Wood also obtained leeside surface pressure data. Those data for three different wings with a two-fold aspect-ratio range are compared in Fig. 3a for nominal values of k_2 and k_3 of 0.40 and 0.13, respectively. According to Fig. 2, the flow type is that of a classic vortex. In Fig. 3b, the data are replotted in similarity form. The hoped-for collapse is evident, with a scatter of roughly ± 5%. Data for a different flow type are shown in Fig. 4. Two wings are compared for nominal values of k_2 and k_3 of 0.67 and 0.12, respectively. The flow type is that of separation bubble plus shock. Again, the data in similarity form collapses as desired.

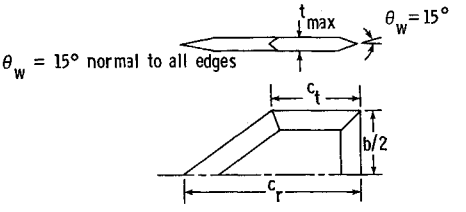

A	b, in.	c_t, in.	c_r, in.	λ	t_{max}, in.	$t_{max}/c_t A$
0.5	4.243	0	16.971	0	0.5	0.058
1.0	6.000	|	12.000	|	|	0.042
2.0	8.486	|	8.486	|	|	0.030
0.5	4.243	5.657	11.314	0.5	|	0.088
1.0	6.000	4.000	8.000	|	|	0.062
2.0	8.485	2.828	5.657	|	|	0.044
4.0	12.000	2.000	4.000	|	|	0.031
0.5	4.243	8.486	8.486	1.0	|	0.118
1.0	6.000	6.000	6.000	|	|	0.083
2.0	8.485	4.243	4.243	|	|	0.059

Fig. 5 Geometrical characteristics of wings in Stallings-Lamb data base.[14]

Force and Moment Correlations for Sharp-Edged Wings

The Stallings and Lamb database[14] has been used for checking similarity for sharp-edged wings. Three families with a wide

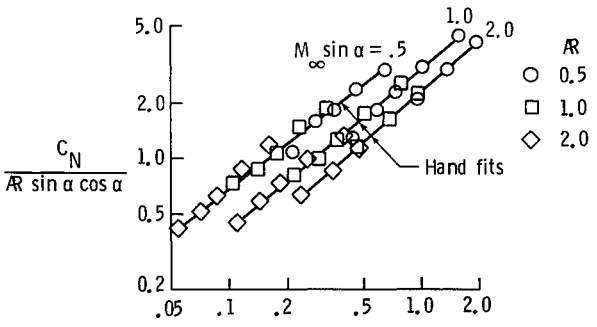

a) Delta wings ($\lambda = 0$)

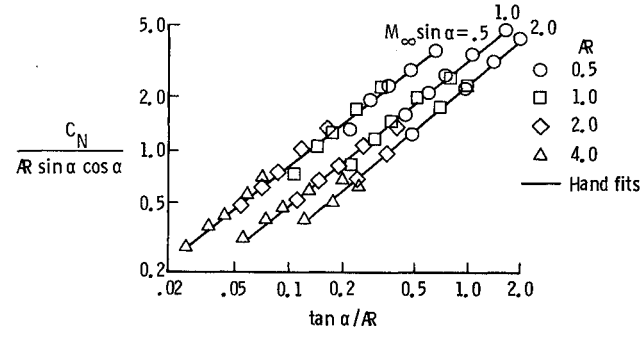

b) Cropped-delta wings ($\lambda = 1/2$)

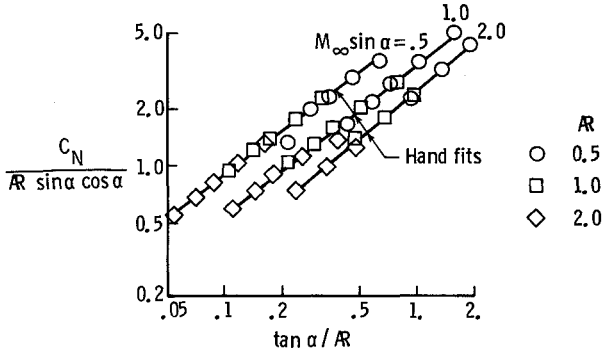

c) Rectangular wings ($\lambda = 1$)

Fig. 6 Correlation of normal-force data for wings in Stallings-Lamb data base.[14]

range of aspect ratios were studied. The geometric characteristics of the wings are given in Fig. 5. It can be seen by considering the airfoil sections and the thickness ratios that the wings in each family (same taper ratio) are affine in planform only. (To be affine, the wings in a family must have identical values of $t_{max}/c_r AR$ as well as similar airfoil sections.) For moderate-to-high supersonic speeds, C_N is only weakly dependent on thickness. However, Nielsen and Goodwin[16] have shown that the axial center-of-pressure location is significantly influenced by wing thickness, depending on the leading-edge sweep.

The Mach number range of the database is from 1.60–4.60, and the angle-of-attack range is from −5 to 60 deg. The aspect-ratio range for the delta and rectangular wings is fourfold from 1/2–2 and for the cropped-delta wings ($\lambda = 1/2$) is eightfold from 1/2–4.

The Stallings and Lamb normal-force data are presented in logarithmic coordinates in Fig. 6 according to Eq. (10). The success of the correlations, even for the rectangular wings, is evident. A surprising feature of the correlations for each family is that they are given by straight lines in logarithmic coordinates and thus can be represented by a one-term power-law expression, i.e.,

$$\frac{C_N}{AR \sin\alpha \cos\alpha} = A(\tan\alpha/AR)^B \tag{20}$$

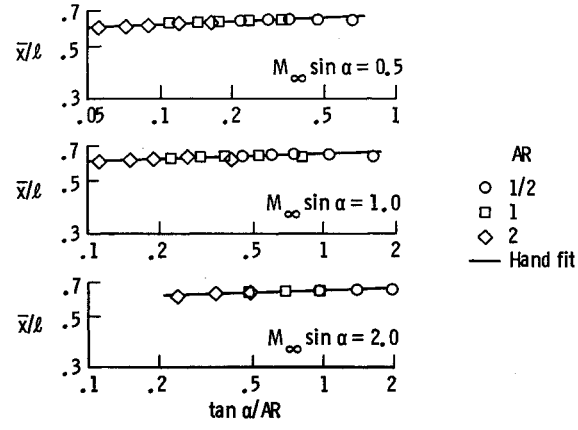

a) Delta wings ($\lambda = 0$)

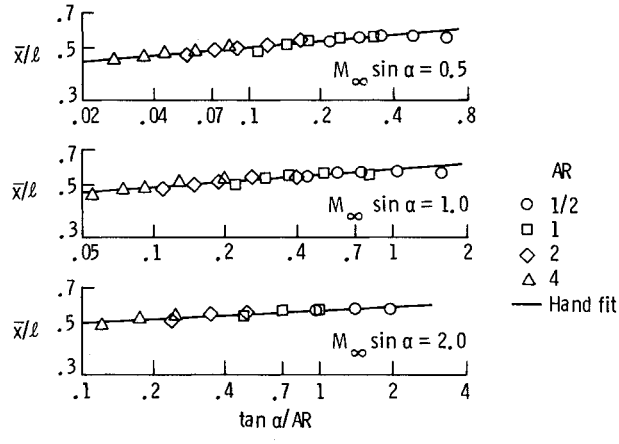

b) Cropped-delta wings ($\lambda = 1/2$)

Fig. 7 Correlation of axial center-of-pressure locations for wings in Stallings-Lamb data base.[14]

where A and B are both functions of $M_\infty \sin\alpha$ only. More will be said about this.

The Stallings and Lamb data for axial and lateral center-of-pressure locations are presented in logarithmic coordinates in Figs. 7 and 8. Axial center-of-pressure data are not presented for the rectangular wings because the nonaffine variation in thickness causes unacceptable scatter. However, it is shown in Ref. 15 that a strip-theory correction suggested by Nielsen and Goodwin[16] can reduce the scatter considerably.

The center-of-pressure correlations of Figs. 7 and 8 are good, and again can be represented as straight lines in logarithmic coordinates. Hence, we can express the correlations as

$$(\bar{x}/\ell) = C(\tan\alpha/AR)^D \tag{21}$$

$$(\bar{y}/s) = E(\tan\alpha/AR)^F \tag{22}$$

where C, D, E, and F are all functions of $M_\infty \sin\alpha$ only. Note that the given correlations were achieved for the Stallings and Lamb wings even though condition (1a) was flagrantly violated.

Force and Moment Correlations for Smooth Bodies

The database obtained by Spencer et al.,[17] Spencer and Phillips,[18] Fournier et al.,[19] and Spencer[20] is particularly useful for checking similarity for smooth bodies. The body planforms are described by a power law with an exponent of 2/3. The body cross sections are elliptic, with ellipticity ratios (span-to-thickness) ranging from 1.0–2.0. Only the $\varepsilon = 1.0$ and $\varepsilon = 2.0$ data will be presented here. The supersonic Mach number range of the tests was from 1.14–2.86. The angle-of-attack

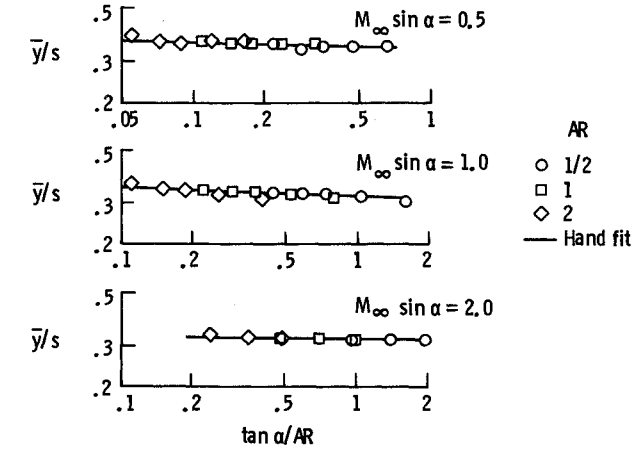

a) Delta wings ($\lambda = 0$)

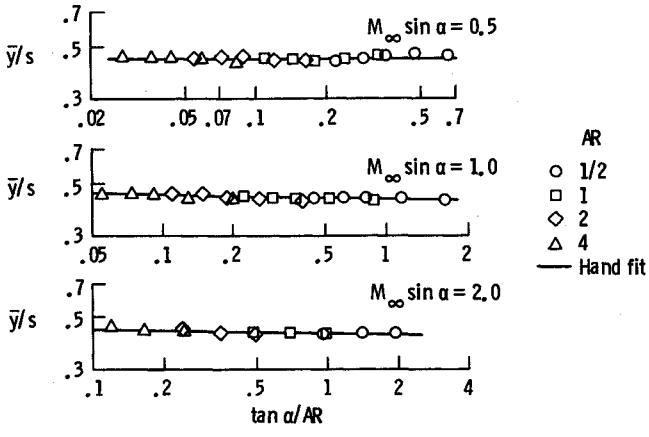

b) Cropped-delta wings ($\lambda = 1/2$)

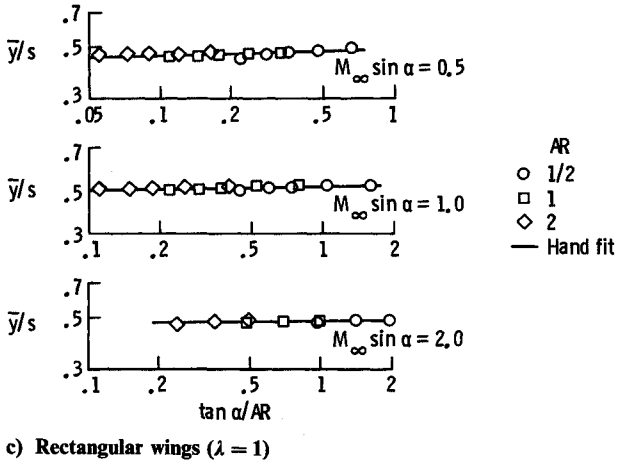

c) Rectangular wings ($\lambda = 1$)

Fig. 8 Correlation of spanwise center-of-pressure locations for wings in Stallings-Lamb data base.[14]

range was from −4 to 26 deg. The aspect ratio range for the $\varepsilon = 2.0$ bodies was from 0.337–0.786 and for the $\varepsilon = 1.0$ bodies 0.294–0.556.

The normal-force correlations according to Eq. (10) are presented in Fig. 9. The correlations are good except for the $\varepsilon = 1.0$ data at $M_\infty \sin\alpha = 0.2$. The scatter for that case can be accounted for by the balance inaccuracy for the angles of attack involved. Note that, as with the sharp-edged wings, the correlations can be represented by a one-term power-law expression [see Eq. (20)].

Correlations of the axial center-of-pressure location according to Eq. (10) are given in Fig. 10 for the $\varepsilon = 2.0$ bodies. The correlations are good and show $\bar{x}/\ell$ to be essentially independent of $\tan\alpha/AR$ and only weakly dependent on $M_\infty \sin\alpha$ for this particular family of bodies.

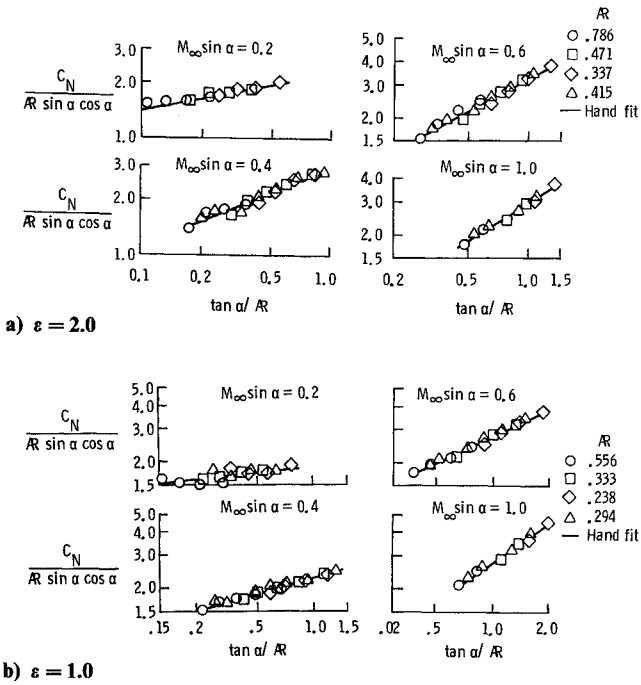

a) $\varepsilon = 2.0$

b) $\varepsilon = 1.0$

Fig. 9 Correlation of normal-force data[17–20] for power-law bodies ($n = 2/3$) with elliptical cross sections.

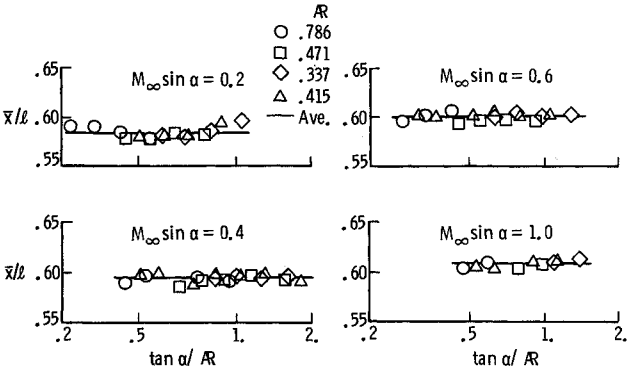

Fig. 10 Correlation of axial center-of-pressure locations for power-law bodies ($n = 2/3$) with elliptical cross sections, $\varepsilon = 2.0$

Discussion of Correlation Results

Normal Force

As shown, all of the normal-force correlations for the three families of sharp-edged wings and the two families of smooth bodies are represented by the one-term power-law expression of Eq. (20). Other data, not presented here, for a variety of slender bodies are also well represented by Eq. (20). Such a representation has apparently not been seen before, and the mathematical basis for it is not understood.

In keeping with the goal of developing engineering design methods, it is worthwhile to examine possible limits for the coefficients A and B. As $M_\infty \sin\alpha \to \infty$, it is expected that the flow will become Newtonian, i.e., C_N will become proportional to $\sin^2\alpha$, with the coefficient of proportionality being independent of M_∞. In order for this to happen, A must tend to a constant and B must tend to one.

For $M_\infty \sin\alpha \to 0$ (with $M_\infty > 1$), it is expected that C_N will be linear in α. There are two limits that will give this behavior. The first occurs if

$$B(0) \neq 0 \tag{23}$$

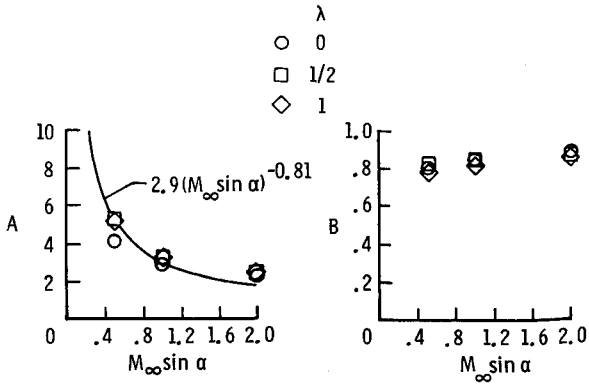

Fig. 11 Coefficients and exponents for normal-force correlations of Stallings-Lamb data.[14]

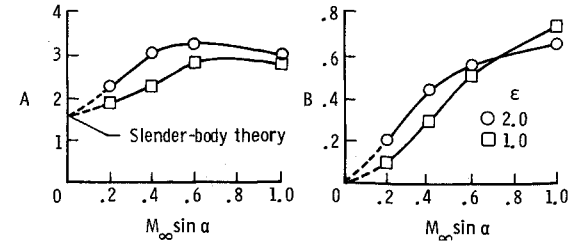

Fig. 12 Coefficients and exponents for normal-force correlations of power-law bodies with elliptical cross sections ($n = 2/3$).

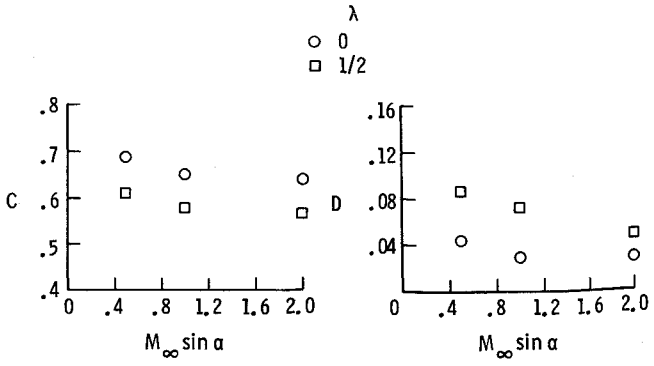

a) Axial center-of-pressure location

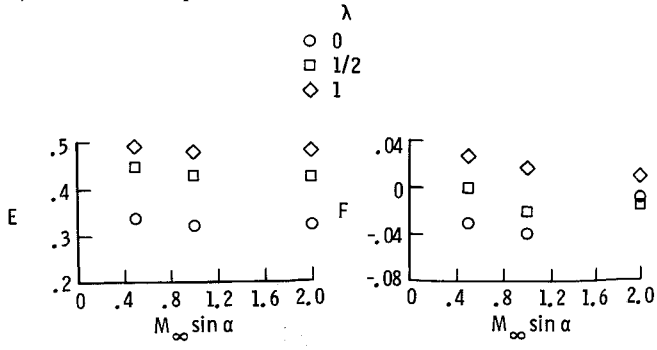

b) Spanwise center-of-pressure location

Fig. 13 Coefficients and exponents for center-of-pressure correlations of Stallings-Lamb data.[14]

If Eq. (23) holds, then for C_N to be linear in α, A must behave as follows:

$$A \sim (M_\infty \sin\alpha)^{-B(0)} \tag{24}$$

so that

$$\frac{C_{N_\alpha}}{AR} \sim (M_\infty AR)^{-B(0)} \tag{25}$$

This first type of limit for small crossflow Mach numbers is exhibited by the sharp-edged wings of Stallings and Lamb.[14] The coefficients A and B are given in Fig. 11 for all three families. Note that B appears to be tending to a finite value of roughly 0.81 for small $M_\infty \sin\alpha$. In addition, B is tending to one and A to a constant for $M_\infty \sin\alpha \to \infty$ as expected.

It is shown in Ref. 15 that the limiting behavior described by Eq. (25) is exhibited by the cropped-delta family. The limiting curve as deduced in Ref. 15 is given in Fig. 11.

The second kind of limit occurs if

$$B(0) = 0 \tag{26}$$

Then for C_N to be linear in α, A must tend to a constant. This type of limit for small crossflow Mach numbers is exhibited by the smooth bodies (Refs. 17–20). The coefficients A and B are given in Fig. 12 for $\varepsilon = 2.0$ and 1.0. Note that B appears to be tending to zero while A appears to be tending to $\pi/2$, which is the slender-body-theory limit for elliptical cross sections. Here too, the coefficients appear to be tending to Newtonian limits.

Center of Pressure

The given center-of-pressure correlations are also represented by one-term power-law expressions [Eqs. (21) and (22)]. The deduced coefficients and exponents for the Stallings and Lamb wings are given in Fig. 13. As noted, it is expected that the flow will become Newtonian as $M_\infty \sin\alpha \to \infty$. For thin flat wings, then $\bar{x}/\ell$ and $\bar{y}/s$ should tend toward the location of the area centroid. For this to happen, the exponents D and F must tend to zero while the coefficients C and E tend toward the area centroid locations. This behavior is suggested by the data of Fig. 13, although the effects of thickness cause the coefficients to shift somewhat upstream from the location of the area centroids.

Conclusions

The similarity parameters deduced by Sychev for inviscid hypersonic flow over slender bodies have been shown to correlate a wide range of supersonic flows over sharp-edged and smooth bodies. Furthermore, it has been shown that the range of applicability of the similarity is far wider than Sychev supposed. For example, the similarity appears to apply for all crossflow Mach numbers and for thin-wing aspect ratios as high as four.

Unexpectedly, one-term power-law expressions are found to fit all of the correlations. It is shown that the power-law expressions tend naturally to the Newtonian limit as $M_\infty \sin\alpha \to \infty$. Furthermore, for $M_\infty \sin\alpha \to 0$, the expression for normal force appears to have two possible limits. The power-law coefficients for thin sharp-edged wings tend to a linear-theory limit, while those for the smooth bodies tend to the slender-body-theory limit. Although the power-law expressions [Eqs. (20–22)] appear to be general, it is not yet clear what the low-crossflow Mach number behavior of the coefficients and exponents will be for any given body.

Acknowledgments

The support of the High Reynolds Number Aerodynamic branch of NASA Langley Research Center under Contract NAS1-18000 is gratefully acknowledged. Helpful discussions with Drs. R. W. Barnwell, J. M. Luckring, and R. M. Hall and Mr. E. C. Polhamus are also gratefully acknowledged.

References

[1]Gentry, A. E., Oliver, W. R., and Smyth, D. N., "The Mark IV Supersonic-Hypersonic Arbitrary Body Program," AFFDL-TR-73-159, Nov. 1973.

[2]Jorgensen, L. H., "Prediction of Static Aerodynamic Characteristics for Slender Bodies Alone and with Lifting Surfaces to Very High Angles of Attack," NASA TR-R-474, Sept. 1977.

[3]Vukelich, S. R., "Aerodynamic Prediction of Elliptically-Shaped Missile Configurations Using Component Build-Up Methodology," AIAA Paper 85-0271, Jan. 1985.

[4]Stoy, S. L. and Vukelich, S. R., "Prediction of Aerodynamic Characteristics of Unconventional Missile Configurations Using Component Build-Up Techniques," AIAA Paper 86-0489, Jan. 1986.

[5]Ashley, H. and Landahl, M., *Aerodynamics of Wings and Bodies*, Addison-Wesley, 1965.

[6]Allen, H. J., "Estimation of the Forces and Moments Acting on Inclined Bodies of Revolution of High Fineness Ratio," NACA RM A9I26, 1949.

[7]Sychev, V. V. "Three-Dimensional Hypersonic Gas Flow Past Slender Bodies at High Angles of Attack," *Journal of Applied Mathematics and Mechanics*, Vol. 24, 1960, pp. 296–306.

[8]Barnwell, R. W., "Extension of Hypersonic, High-Incidence, Slender-Body Similarity to Lower Mach Numbers," *AIAA Journal*, Vol. 25, Nov. 1987, pp. 1519–1522.

[9]Tsien, H. S., "Similarity Laws of Hypersonic Flow," *Journal of Mathematical Physics*, Vol. 25, 1946, pp. 247–251.

[10]Hamaker, F. M., Neice, S. E., and Wong, T. J., "The Similarity Law for Hypersonic Flow and Requirements for Dynamic Similarity of Related Bodies in Free flight," NACA Rept. 1147, 1953.

[11]Hayes, W. D., "On Hypersonic Similitude," *Quarterly of Applied Mathematics*, Vol. 5, No. 1, April 1947, pp. 105–106.

[12]Smith, J. H. B., "A Theory of the Separated Flow from the Curved Leading Edge of a Slender Wing," Aeronautical Research Council Reports and Memorandum No. 3116, Nov. 1957.

[13]Miller, D. S. and Wood, R. M., "Lee-Side flow over Delta Wings at Supersonic Speeds," NASA TP 2430, June 1985.

[14]Stallings, R. L., Jr., and Lamb, M., "Wing-Alone Aerodynamic Characteristics for High Angles of Attack at Supersonic Speeds," NASA TP 1889, July 1981.

[15]Hemsch, M. J., "Engineering Analysis of Slender-Body Aerodynamics Using Sychev Similarity Parameters," AIAA Paper 87-0267, Jan. 1987.

[16]Nielsen, J. N and Goodwin, F. K., "Preliminary Method for Estimating Hinge Moments of All-Movable Controls," Nielsen Engineering and Research Inc., Mountain View, CA, TR 268, March 1982.

[17]Spencer, B., Jr., Phillips, W. P., and Fournier, R. H., "Supersonic Aerodynamic Characteristics of a Series of Bodies Having Variations in Fineness Ratio and Cross-Sectional Ellipticity" NASA TN D-2389, Aug. 1964.

[18]Spencer, B., Jr. and Phillips, W. P., "Transonic Aerodynamic Characteristics of a Series of Bodies having Variations in Fineness Ratio and Cross-Sectional Ellipticity" NASA TN D-2622, Feb. 1965.

[19]Fournier, R. H., Spencer, B., Jr., and Corlett, W. A., "Supersonic Aerodynamic Characteristics of a Series of Related Bodies with Cross-Sectional Ellipticity," NASA TN D-3539, 1966.

[20]Spencer, B., Jr., "Transonic Aerodynamic Characteristics of a Series of Related Bodies with Cross-Sectional Ellipticity," NASA TN D-3203, 1966.